



The important roles and molecular mechanisms of annexin A₂ autoantibody in children with nephrotic syndrome

Qing Ye^{1#}, Yingying Zhang^{2#}, Jieqiu Zhuang³, Ye Bi³, Hong Xu⁴, Qian Shen⁴, Jialu Liu⁴, Haidong Fu², Jingjing Wang², Chunyue Feng², Xiaoxiao Tang², Fei Liu², Weizhong Gu⁵, Fei Zhao⁶, Jianjiang Zhang⁷, Yuanhan Qin⁸, Shiqiang Shang¹, Hongqiang Shen¹, Xuejun Chen¹, Huijun Shen², Aimin Liu², Yonghui Xia², Zhihong Lu², Qiang Shu⁹, Jianhua Mao²

¹Department of Clinical Laboratory, The Children's Hospital of Zhejiang University School of Medicine, National Clinical Research Center for Child Health, Hangzhou, China; ²Department of Nephrology, The Children's Hospital of Zhejiang University School of Medicine, National Clinical Research Center for Child Health, Hangzhou, China; ³Department of Pediatric Nephrology, The Second Affiliated Hospital and Yuying Children's Hospital of Wenzhou Medical University, Wenzhou, China; ⁴Department of Nephrology, Children's Hospital of Fudan University, National Pediatric Medical Center of China, Shanghai, China; ⁵Department of Pathology, The Children's Hospital of Zhejiang University School of Medicine, National Clinical Research Center for Child Health, Hangzhou, China; ⁶Department of Nephrology, Children's Hospital of Nanjing Medical University, Nanjing, China; ⁷Department of Pediatrics, First Affiliated Hospital of Zhengzhou University, Zhengzhou, China; ⁸Department of Pediatric Nephrology, The First Affiliated Hospital of Guangxi Medical University, Nanning, China; ⁹Department of Thoracic and Cardiovascular Surgery, The Children's Hospital of Zhejiang University School of Medicine, National Clinical Research Center for Child Health, Hangzhou, China

Contributions: (I) Conception and design: J Mao, Q Shu; (II) Administrative support: J Mao, Q Shu; (III) Provision of study materials or patients: Q Ye; (IV) Collection and assembly of data: Q Ye, Y Zhang, J Zhuang, Y Bi, H Xu, Q Shen, J Liu, H Fu, J Wang, C Feng, X Tang, F Liu, W Gu, F Zhao, J Zhang, Y Qin, H Shen, A Liu, Y Xia, Z Lu; (V) Data analysis and interpretation: Q Ye, Y Zhang; (VI) Manuscript writing: All authors; (VII) Final approval of manuscript: All authors.

[#]These authors contributed equally to this work.

Correspondence to: Jianhua Mao. Department of Nephrology, the Children's Hospital, Zhejiang University School of Medicine, National Clinical Research Center for Child Health, Hangzhou 310052, China. Email: maojh88@zju.edu.cn; Qiang Shu. Department of Thoracic and Cardiovascular Surgery, the Children's Hospital, Zhejiang University School of Medicine, National Clinical Research Center for Child Health, Hangzhou 310052, China. Email: shuqiang@zju.edu.cn.

Background: In recent years, B-cell dysfunction has been found to play an important role in the pathogenesis of primary nephrotic syndrome (PNS). B cells play a pathogenic role by secreting antibodies against their target antigens after transforming into plasma cells. Therefore, this study aimed to screen the autoantibodies that cause PNS and explore their pathogenic mechanisms.

Methods: Western blotting and mass spectrometry were employed to screen and identify autoantibodies against podocytes in children with PNS. Both *in vivo* and *in vitro* experiments were used to study the pathogenic mechanism of PNS. The results were confirmed in a large multicenter clinical study in children.

Results: Annexin A₂ autoantibody was highly expressed in children with PNS with a pathological type of minimal change disease (MCD) or focal segmental glomerulosclerosis without genetic factors. The mouse model showed that anti-Annexin A₂ antibody could induce proteinuria *in vivo*. Mechanistically, the effect of Annexin A₂ antibody on the Rho signaling pathway was realized through promoting the phosphorylation of Annexin A₂ at Tyr24 on podocytes by reducing its binding to PTP1B, which led to the cytoskeletal rearrangement and damage of podocytes, eventually causing proteinuria and PNS.

Conclusions: Annexin A₂ autoantibody may be responsible for some cases of PNS with MCD/FSGS in children.

Keywords: Chronic kidney disease; nephrotic syndrome; pediatric nephrology; podocyte; cytoskeleton

Submitted Jul 23, 2021. Accepted for publication Sep 01, 2021.

doi: 10.21037/atm-21-3988

View this article at: <https://dx.doi.org/10.21037/atm-21-3988>

Introduction

Primary nephrotic syndrome (PNS) is a clinical syndrome caused by increased plasma protein permeability of the glomerular filtration membrane which can lead to heavy proteinuria and a series of pathological changes (1). As a common type of nephrosis in children, PNS has an incidence rate of 1.15 to 50 per 10,000 children depending on nationality and ethnicity (1-3). Although steroid therapy proves effective for most patients, about 10% to 20% of children with PNS acquire steroid resistance, which is defined as steroid-resistant nephrotic syndrome (SRNS) (4). Between 8% and 35% of children with SRNS progress to end-stage renal disease within 5 years of diagnosis, and this proportion rises to between 24% and 66% within 15 years (5-9). Unfortunately, the pathogenesis of this disease is still not fully understood. According to Ali *et al.*'s report, no proteinuria was found in kidneys transplanted from patients with refractory minimal change disease (MCD), suggesting that the pathogenic factors of MCD are mainly related to the internal systemic environment rather than the kidney itself (10). Further, with the exception of those with certain genetic defects (11), children with SRNS can see an improvement in their condition after treatment with steroids and immunosuppressants, which indirectly evidences the close relationship between PNS/SRNS and immunity.

T-cell dysfunction is a classic theory of the pathogenesis of MCD. There are a number of pieces of evidence supporting the idea that T-cell dysfunction plays a role in MCD. For instance, spontaneous remission of nephrotic syndrome has been reported in some patients with MCD complicated with measles (the measles virus can significantly inhibit cellular immunity) (12). Furthermore, cyclosporine and tacrolimus are effective in managing MCD as they can selectively inhibit T lymphocytes. Studies have also shown that injecting T-lymphocyte culture supernatant from patients with MCD can induce proteinuria in rats (13,14). Moreover, patients with Hodgkin's disease and thymoma, both of which are associated with T-lymphocyte dysfunction, have a higher possibility of developing nephrotic syndrome-related complications. A number of studies have also confirmed that abnormalities in the

quantity and functions of T lymphocytes are closely associated with the onset of MCD (15-18). However, T-cell abnormalities fail to explain the pathogenesis of PNS completely, as therapies targeting T cells are not always effective.

In recent years, B-cell dysfunction has also been found to play an essential part in PNS (19,20). However, aside from that in membranous nephropathy, the target antigen of pathologic B cells in children with PNS remains unclear. MCD and focal segmental glomerular sclerosis (FSGS) are generally considered to be caused by the loss or change of podocyte function, which leads to podocyte disease characterized by heavy proteinuria (2). As the epithelial cells of the visceral layer of the glomerular capillary, podocytes are terminally differentiated cells located on the outer surface of the glomerular basement membrane. Podocytes function as the final barrier to protein loss, and their damage usually results in heavy proteinuria (21,22). Therefore, in the present study, we screened autoantibodies in children with PNS in order to explore whether an autoantibody against podocytes exists and identify the target antigen for any such antibody, its effects, and pathogenic mechanism.

We present the following article in accordance with the ARRIVE reporting checklist (available at <https://dx.doi.org/10.21037/atm-21-3988>).

Methods

Screening and identification of podocyte autoantibodies in children with PNS (23)

To identify the target antigen of the IgG-type autoantibody specific against podocytes in the serum of children with PNS, human podocytes were obtained. The total protein of the podocytes was extracted for SDS-PAGE. Two sets of SDS-PAGE were conducted in parallel, with one used for Coomassie Brilliant Blue staining and the other transferred to a nitrocellulose membrane, to which IgG antibodies purified from the serum of children with PNS were added for western blotting (IgG antibodies were purified from the serum of children with PNS in whom the presence of IgG autoantibodies specific against podocytes had been verified

via mouse podocyte immunofluorescence. Our study included patients with initial onset nephrotic syndrome selected at random. None of the patients had received treatment before autoantibody testing). The samples loaded onto two gels were in complete correspondence. Coomassie Brilliant Blue-stained bands corresponding to positive bands in western blot were selected for mass spectrometry to identify the target antigen, and the results were verified via western blotting using the corresponding recombinant target antigen and its antibody. After the target antigen had been confirmed, a laser scanning confocal microscope was used to observe whether it would co-localized with its autoantibody in the glomerular podocytes of three children with PNS. After that, to determine whether the autoantibody against the target antigen could be sensitized in the glomerular podocytes of children with PNS, the IgG antibodies were eluted from the renopuncture tissues and hybridized with the target antigen *in vitro* (24). The 20 patients initially subjected to autoantibody screening were newly diagnosed, untreated children with nephrotic syndrome and were selected at random.

A prospective multi-center study to examine the clinical application value of Annexin A₂ autoantibody

Children aged 0 to 18 years with initial onset nephrotic syndrome without genetic factors who were admitted to one of six hospitals (The Children's Hospital of Zhejiang University School of Medicine, the Second Affiliated Hospital and Yuying Children's Hospital of Wenzhou Medical University, Children's Hospital of Fudan University, Children's Hospital of Nanjing Medical University, the First Affiliated Hospital of Zhengzhou University and the First Affiliated Hospital of Guangxi Medical University) were included in this national multicenter clinical study from January 1, 2017, to October 1, 2019, without sex preference. Annexin A₂ autoantibody in the children were detected by western blotting. The patients also underwent second-generation gene sequencing to exclude those with inherited nephrotic syndrome.

This study is registered in the Chinese Clinical Trial Registry (registration no. ChiCTR1900027202). The ethics committee of The Children's Hospital of Zhejiang University School of Medicine approved the study (2019-IRB-139). Informed consent was obtained from the parents/guardians of each patient after they had received a full explanation of the purpose of the study. All procedures involving human participants were performed in accordance

with the Declaration of Helsinki (as revised in 2013).

Western blotting of Annexin A₂ autoantibody

Annexin A₂ protein (200 µg/mL, #ab93005, Abcam) was spotted onto a 0.8-µm pore size nitrocellulose membrane (Sartorius, Germany) using a chip sampling apparatus (AD1500, BioDot). Biotin-labeled mouse anti-human IgG (ThermoFisher) and 56 °C-inactivated serum were also spotted onto the nitrocellulose membranes as a positive and negative control, respectively. The nitrocellulose membrane spotted with Annexin A₂ protein was soaked in a 5% bovine serum albumin (BSA) sealing solution for 1 hour (Tween/Tris-buffered saline with a pH of 7.4 was used as the buffer system.) and then oven dried. Then, the membrane was fixed in the groove of a polyvinyl chloride assay plate, and 300 µL of serum or a 30-fold dilution of serum from patients with PNS was added to the groove of the assay plate. After subjecting the membrane to incubation and washing with Tris buffer five times, we added 300 µL of biotin anti-human IgG antibody complex to the assay plate. After further incubation and washing, we washed the assay plate with running water and read it with a scanner. The amount of Annexin A₂ antibody was determined by detecting the optical density value of the positive point of the reaction. Patients with nephrotic syndrome were used as the disease group, while the negative control group comprised healthy people and patients with common kidney diseases such as IgA nephropathy, purpuric nephritis, allergic purpura, and hematuria. From the optical density value of the reaction point, the receiver operating characteristic (ROC) curve was drawn, and the cut-off point was determined according to the Youden index. Results above the cut-off point were reported as positive and those under the cut-off point were reported as negative.

Immunoglobulin elution and immunoblotting with Annexin A₂ protein in renal biopsy specimens

Frozen renal biopsy specimens from patients with PNS who were positive for anti-Annexin A₂ antibodies were selected to obtain a sufficient amount of IgG for analysis. The renal biopsy tissues were cut into 20-µm-thick sections. They were collected in a microcentrifuge tube and washed with PBS several times to remove residual OCT compounds. Then, the renal biopsy tissues were incubated with 60 µL citrate buffer (25 mM, pH 3.2) for 20 minutes, and the eluent was collected following centrifugation. After that,

the tissues were incubated with 40 μ L citrate buffer (25 mM, pH 2.5) for 20 minutes, and once more, the eluent was collected following centrifugation. A total of 100 μ L eluent was collected and neutralized with a small amount of 2M NaOH and 2M Tris, with the pH value adjusted to 7.3. The eluted IgG was used as a primary antibody and was reacted with the Annexin A₂ protein band isolated from the human kidney tissue and recombinant Annexin A₂ protein. IgG and IgG4 antibodies against Annexin A₂ in the eluent were detected using anti-IgG and anti-IgG4 secondary antibodies, respectively. The specific experimental parameters were as follows: 10% gel for electrophoresis; 250 mA, 2.5 hours for transfer; the primary antibody was incubated at 4 °C overnight; horseradish peroxidase (HRP)-conjugated goat anti-rabbit IgG and HRP-conjugated IgG4 antibody were used for secondary antibody incubation at room temperature for 1 hour.

Immunofluorescence staining for local co-localization of Annexin A₂ in podocytes and IgG in the glomerulus

Fresh kidney biopsy specimens were cut into 4- μ m-thick slices and fixed in 4% paraformaldehyde (PFA) for 20 minutes. After being blocked with 5% BSA at room temperature for 1 hour, the kidney sections were incubated overnight at 4 °C with the following primary antibodies: FITC-IgG antibody (#318F190927, DAKO), nephrin goat antibody (0.4 μ g/mL; #AF3159, R&D Systems), and Annexin A₂ rabbit antibody (20 μ g/mL; #ab41803, Abcam). After that, the sections were incubated with Alexa Fluor 594-conjugated donkey anti-rabbit (2 μ g/mL; A21207, Life Technology) or donkey anti-goat secondary Abs (2 μ g/mL; A11058, Life Technology) for 1 hour at room temperature. Finally, images were taken under a Nikon A1 confocal laser microscope.

Effects of Annexin A₂ antibody on mouse kidneys

Five male BALB/c mice were each injected intravenously with 100 μ g of rabbit polyclonal Annexin A₂ antibody (ab41803, Abcam) and included as the experimental group. The antibody dose was based on the literature and preliminary experimental results (24,25). As the control group, 5 male BALB/c mice were injected intravenously with an equal amount of rabbit IgG polyclonal antibody-isotype control (ab37415, Abcam). The mice were kept in a metabolic cage for 1 week and urine samples were collected every 24 hours. A total of 7 urine samples from each mouse

were collected, and the 24-hour urine protein content was detected. After 7 days, the mice were anesthetized with 4% chloral hydrate and sacrificed. The kidneys were removed and stored at -80 °C ahead of hematoxylin-eosin (HE) staining, trichrome staining, immunofluorescence staining, and transmission electron microscope (TEM) observation. The specific experimental methods are detailed in our previous paper (26). All animal experiments were performed under a project license (No. 20744) granted by Zhejiang University School of Medicine, and in compliance with the national guidelines for the care and use of animals.

Immunofluorescence staining

Mouse kidney tissues were cut into 4- μ m-thick slices using a Leica frozen slicer. The kidney slices were washed twice with phosphate-buffered saline (PBS) for 5 minutes at room temperature, blocked with 3% BSA at room temperature, and then incubated overnight at 4 °C with the primary antibodies for nephrin (0.4 μ g/mL; #AF3159, RD), ZO-1 (7 μ g/mL; #21773-1-AP, Proteintech), WT1 (4.8 μ g/mL; #ab89901, Abcam), and desmin (1.2 μ g/mL; 16520-1-AP, Proteintech). On the second day, the kidney slices were washed 3 times with PBS, for 5 minutes each time, and then incubated with Alexa Fluor 594-conjugated donkey anti-rabbit (2 μ g/mL; A21207, Life Technology) or donkey anti-goat secondary Abs (2 μ g/mL; A11058, Life Technology) for 1 hour at room temperature. Finally, images were taken under a Nikon A1 confocal laser microscope.

Effects of Annexin A₂ antibody on podocytes

Anti-Annexin A₂ antibody was added to the podocyte culture medium for 12 h and the following were detected: the adhesion, migration, and phagocytosis ability of podocytes; structural changes in the podocyte cytoskeleton protein F-actin; changes in the expression of Cdc42, Rac1/2/3, and RhoA, as key molecules in the Rho signaling pathway; and changes in the phosphorylation level of Annexin A₂ protein.

Detecting the adhesion ability of podocytes

Cell matrix adhesion is essential for the maintenance of epithelial tissue integrity. Podocytes, which are a key component of the glomerular filtration barrier, are exposed to permanent transcapillary filtration pressure and therefore must adhere tightly to the underlying glomerular basement membrane. After synchronization for 12 hours, mouse

podocyte clone-5 (MPC5) cells differentiated at 37 °C from different groups were seeded into 6-well plates at a density of 0.4×10^6 . After 1 hour, the cells were washed 3 times with cold PBS to remove those that were unattached. The cells were then fixed with PFA for 20 minutes and washed 3 times with PBS. Under a microscope, the adherent cells in each well were counted in 12 randomly selected, high magnification views. Three wells were counted for each group, and counting was repeated 3 times. The immortalized mouse podocyte cell line was donated by Prof. Mundel (Goldfinch Bio).

Detecting the migration ability of podocytes

Podocytes are a contractile and mobile cell type, and their migration ability is extremely important to their adaption to environmental changes. To detect the migration ability of podocytes, 8- μ m Transwell chambers were suspended on a 24-well plate, and 100 μ L collagen was added to each chamber. After synchronization for 12 hours, MPC5 cells differentiated at 37 °C from different groups were seeded into 24-well plates at a density of 0.2×10^5 . After 7 hours, the non-migrated cells on the cell membrane were gently wiped off with a cotton swab, and the remaining cells were washed 3 times with PBS and fixed with PFA for 20 minutes. The cells were then stained with 1% purple crystals for 10 minutes and washed with distilled water. The cells in 12 high magnification views were randomly observed and counted. Counting was repeated 3 times.

Detecting the phagocytosis ability of podocytes

Endocytosis is necessary for podocytes to regenerate their slit diaphragm. Abnormal endocytosis is related to nephrotic syndrome. MPC5 cells differentiated at 37 °C from different groups were seeded into 24-well plates. When the confluency reached about 80%, the cells were synchronized for 12 hours. The medium was subsequently discarded and 50 μ g/mL FITC-transferrin was added to each well. The cells were then incubated at 37 °C for 5 hours, after which the transferrin was discarded and the cells were washed, first with citrate buffer (containing deferoxamine mesylate) 3 times and then with PBS 3 times. After that, the cells were fixed with PFA for 20 minutes and stained with DAPI for 10 minutes. Images were taken with a Nikon A1 Ti laser scanning confocal microscope. Six high-magnification views were randomly selected for each well, and six wells were selected for each group. The fluorescence intensity was

measured, and the measurements were repeated 3 times.

Detecting Rho signaling pathway

Podocytes were treated with anti-Annexin A₂ antibody for 24 hours, after the medium was removed and the podocytes washed 3 times with cold PBS. Total protein was extracted from the podocytes with RIPA lysis buffer (#89900, ThermoFisher) containing protease inhibitor (1:200, ab20111, Abcam), and the Pierce BCA Protein Assay Kit (#23227, ThermoFisher) was used for protein quantification. Equal amounts of protein (20 μ g) were separated by 10% SDS-PAGE before being transferred to PVDF membranes (#88518, ThermoFisher). For phospho-Annexin A2 detection, 5 mM phos-tag (#F4002, APEX BIO) was added into the gel, and protein extracts were separated by 6–8% SDS-PAGE at 4 °C. The membranes were blocked with 5% BSA for 1 hour at room temperature and then incubated overnight at 4 °C in a 1:1000 dilution of Cdc42 (2466, 1:1,000, CST), Rac1/2/3 (1:1,000, #2465, CST), and RhoA (1:1,000, #2117, CST). On the second day, after being washed 3 times with Tris-buffered saline with Tween-20 (TBST), the membranes were incubated with HRP-conjugated goat anti-rabbit/mouse IgG antibody (1:10,000, SA0000-1, SA0000-2, Proteintech) for 1 to 2 hours at room temperature. Then, after 3 washes with TBST, images were captured using the Bio-Rad Imaging System.

RhoA/Rac1/Cdc42 Combo Activation Assay Kit

After treatment with anti-Annexin A₂ antibody, podocytes were washed twice with ice-cold PBS, and total protein was extracted from the podocytes using 1X Assay Buffer. Then, 40 μ L of resuspended RhoA receptor-binding domain or PAK1 p21-binding domain beads were added to each sample for 1 hour with gentle agitation at 4 °C. The beads were pelleted through centrifugation at 14,000 \times g for 10 seconds, and the supernatant was aspirated, with care taken to avoid disturbing/removing the bead pellets. The bead pellets were washed 3 times with 0.5 mL 1X Assay Buffer, centrifuged, and aspirated each time. After the final wash, the beads were pelleted, and the supernatant was completely and carefully removed. The bead pellets were resuspended with 40 μ L 4X reducing SDS-PAGE sample buffer and boiled for 5 minutes at 100 °C. Protein extracts (20 μ g) were separated by 10% SDS-PAGE, before being transferred to PVDF membranes (#88518, ThermoFisher).

The membranes were blocked with 5% BSA for 1 hour at room temperature and then incubated in a 1:1,000 dilution of Cdc42, Rac1/2/3, and RhoA overnight at 4 °C (ab211168, Abcam). On the second day, after being washed 3 times with TBST, the membranes were incubated with HRP-conjugated goat anti-rabbit/mouse IgG antibody (1:10,000, SA00001-1, SA00001-2, Proteintech) for 1 to 2 hours at room temperature. After 3 washes with TBST, images were captured using the Bio-Rad Imaging System.

Effects of the Tyr24 phosphorylation of Annexin A₂ on the cytoskeleton and functions of podocytes

Annexin A₂ Tyr24 was mutated to glutamic acid to simulate phosphorylation (Y24E) and to alanine to simulate dephosphorylation (Y24A), and these mutants were subsequently overexpressed in podocytes (27,28). The adhesion, migration, and phagocytosis abilities of podocytes were detected after Tyr24 hyperphosphorylation of Annexin A₂. Immunofluorescence staining was used to detect podocyte cytoskeleton proteins, and western blotting and pulldown were adopted to detect changes in the expression and activities of Cdc42 and Rac1, as key molecules in the Rho-associated kinase signaling pathway (29).

Identification of PTP1B as an Annexin A₂-interacting protein

MPC5 cells were cross-linked with 10% formaldehyde for 10 minutes. The cross-linking reaction was quenched with 2 M of glycine (pH 7.4) for 5 minutes. Cells were lysed in lysis buffer (50 mM Tris-HCl, pH 7.4, 3MKCl, 500 mM EDTA, 0.1% Triton X-100) supplemented with protease inhibitor cocktail. After sonication, cell lysates were pre-cleared with Dynabeads™ Protein A (#10001D, ThermoFisher) for 1 hour at 4 °C. The lysates were then incubated with anti-Annexin A₂ antibody (5 µg) overnight at 4 °C. The protein A beads were washed with lysis buffer 3 times and then incubated with antigen-antibody for 4 to 6 hours at 4 °C. The bead-bound protein complex was boiled for 5 minutes in SDS sample buffer at 98 °C and loaded into SDS-PAGE gel. The primary antibodies used were anti-Annexin A₂ antibody (1 µg/mL; #ab41803, Abcam) and anti-PTP1B antibody (0.5 µg/mL; #ab244207, Abcam). After primary antibody incubation, the protein complex was incubated with HRP-conjugated goat anti-rabbit IgG antibody (1:10,000; #SA00001-2, Proteintech) and another secondary antibody (0.04 µg/mL; #ab131366,

Abcam), respectively.

Annexin A₂ elution and western blotting detection of Annexin A₂ on the surface of podocytes

MPC5 cells were pre-treated with 20 µg/mL Annexin A₂ antibody after 12 hours of synchronization. The cells were immediately equilibrated to 4 °C on ice for 5 minutes before being rinsed with ice-cold PBS and treated with 10 mM EGTA in PBS (600 µL/6 cm dish) for 30 minutes. The eluates were collected after centrifugation at 500 g for 10 minutes. Total protein extracts were quantified using a BCA protein assay kit (#23227, ThermoFisher) before being separated by 10% SDS-PAGE and then transferred to PVDF membranes (250 mA/2.5 h). After being blocked with 5% non-fat milk for 1 hour at room temperature, the membranes were incubated with primary Annexin A₂ antibody (1 µg/mL; #ab41803, Abcam) and then with secondary HRP-conjugated goat anti-rabbit IgG antibody (1:10,000; #ab6721, Abcam). Signals were detected with an enhanced chemiluminescence (ECL) kit (#34095, ThermoFisher). Images were captured using the Bio-Rad Imaging System.

Indirect immunofluorescence detection of total Annexin A₂ and Annexin A₂ on the surface of podocytes

Podocytes were pre-treated with 20 µg/mL Annexin A₂ antibody after 12 hours of synchronization. The cells were fixed with 4% PFA for 20 minutes and permeated with 0.2% Triton X-100 for 20 to 30 minutes (when Annexin A₂ was only detected on the cell surface, permeation with 0.2% Triton X-100 was not carried out). After being blocked with 5% BSA for 1 hour at room temperature, the cells were incubated with anti-Annexin A₂ antibody (20 µg/mL; #ab41803, Abcam) at 4 °C overnight, which was followed by incubation with Alexa Fluor 594-conjugated donkey anti-rabbit secondary Abs (2 µg/mL, #a21207, Life Technology) for 1 hour at room temperature. Images were taken with a Leica microscope (Leica DM4000).

Statistical analysis

Variables were compared between the two groups by chi-square test. Normally distributed measurement data were represented as the mean ± standard deviation (SD), while data that were not normally distributed were represented by the median (range). For comparisons between three groups

in which the samples were independent and normally distributed and had equal variances, one-way analysis of variance (ANOVA) was adopted; for comparisons between two groups, the least significant difference (LSD) test was adopted. Continuous variables which lacked a normal distribution and equal variance were compared by non-parametric Mann-Whitney U test. The fluorescent stained images were subjected to fluorescence quantitative analysis using Image J. A grayscale analysis of western blotting quantitative analysis results was carried out with Image J. $P < 0.05$ was defined as statistically significant (* $P < 0.05$, ** $P < 0.01$, *** $P < 0.001$, **** $P < 0.0001$). All statistical analyses were processed in SPSS 22.0 statistical software (IBM Corporation, USA).

Results

The presence of IgG autoantibody against podocytes in the serum of children with PNS

To determine the presence of autoantibodies specific against renal podocytes in children with PNS, serum was collected from 20 children with PNS. The IgG-type autoantibody specific against podocytes was detected in 14 out of 20 children with PNS (Figure S1).

Annexin A₂ in podocytes serve as the main target antigen for the autoantibodies in children with PNS

To further clarify the target antigen for the IgG-type autoantibody against podocytes in the serum of children with PNS, the serum of children with PNS was used as the primary antibody (the presence of IgG autoantibody against podocytes had been verified in 14 patients via human podocyte immunofluorescence) for western blotting detection, with the total protein of human podocytes used as an antigen. The darkest bands common to all the patients were selected for mass spectrometry analysis. Annexin A₂ was identified as the target antigen. Subsequently, the commercial recombinant Annexin A₂ protein and anti-Annexin A₂ antibody were purchased to verify the results of mass spectrometry identification via western blotting. Together, the results showed that Annexin A₂ in podocytes acts as the main target antigen for the autoantibody in children with PNS. The experimental results are shown in Figure S2.

Detection of Annexin A₂ autoantibody can identify children with autoimmune nephrotic syndrome induced by non-genetic factors

Annexin A₂ autoantibody was detected in 596 children with PNS without genetic factors. A positive result was reported in 106 of these cases, which translated to a detection rate of 17.8%. In contrast, the autoantibody was not found in children with Henoch-Schonlein purpura nephritis (n=344), IgA nephropathy (n=277), isolated proteinuria (n=150), or lupus nephritis (n=120), or in the healthy children (n=300) (Figure 1A). Renal biopsy was conducted in 61 of the 106 cases (including 33 cases of SRNS and 28 cases of FRNS/SDNS) that were positive for Annexin A₂ autoantibody, and the pathological type of all of these cases was MCD/FSGS.

The median hospital stay was significantly longer for children with PNS who were positive for anti-Annexin A₂ antibody than for those with a negative result (17 vs. 12 days, $Z = -2.539$, $P = 0.011$). Total trace protein in urine (M-TP) ($Z = -2.341$, $P = 0.029$) and U-IgG/Cr ($Z = -2.543$, $P = 0.011$) were also significantly increased in the children in the positive group, with medians of 2,550.6 vs. 1,706.0 mg/L and 11.75 vs. 6.5, respectively (Figure 1B). When immunosuppressants were administered to the children with PNS who were positive for Annexin A₂ autoantibody, in all 30 children observed, the level of anti-Annexin A₂ antibody gradually decreased *in vivo*, which was accompanied by a continuous decrease in the 24-hour urine protein level and an increase in serum albumin. The typical change pattern is displayed in Figure 1C,1D.

Autoantibody against glomerular podocyte Annexin A₂ protein is present in the kidney tissues of children with PNS

Although anti-Annexin A₂ antibody was detected in the serum of PNS children, it was still unclear whether anti-Annexin A₂ antibody can deposit in the glomerulus and lead to renal podocyte damage. In an effort to explore this, we subjected the kidney tissues of children with PNS whose serum tested positive for anti-Annexin A₂ antibody to immunofluorescence staining and then eluted the IgG antibodies in the glomerulus for identification. The results showed that nephrin—which is expressed on the podocyte foot process slit diaphragm—Annexin A₂ in podocytes, and IgG could locally co-localized in the glomerulus

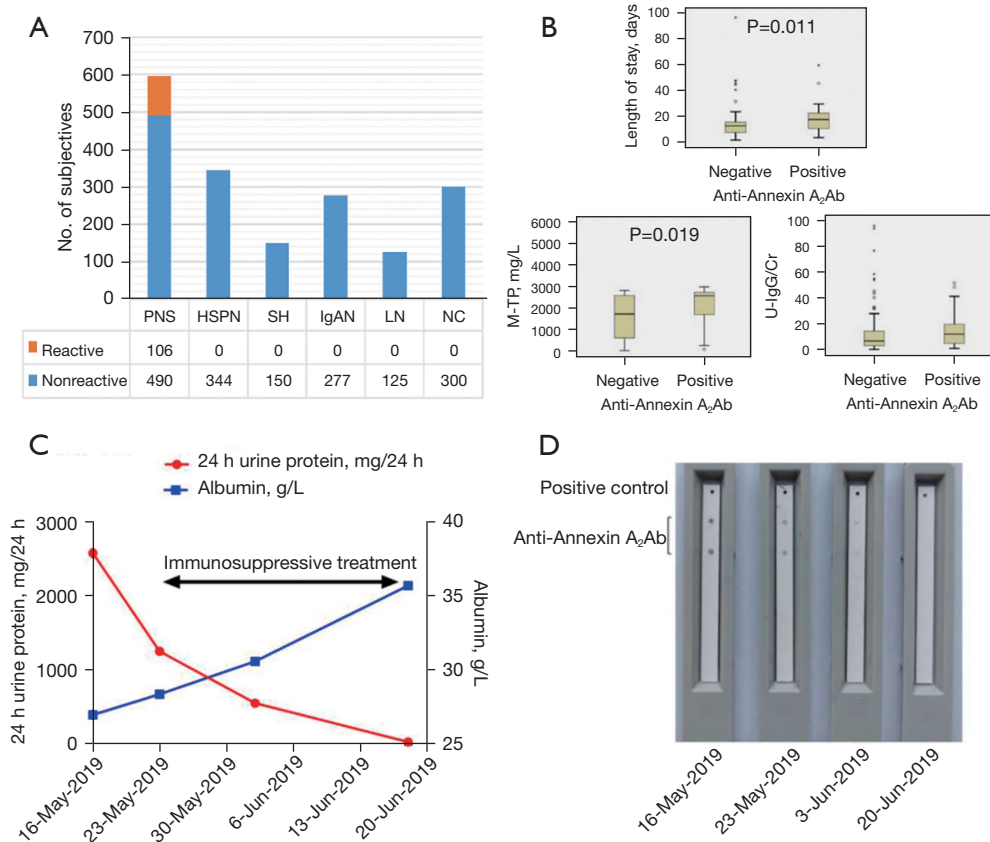


Figure 1 Annexin A₂ autoantibodies in children with PNS are associated with laboratory parameters, hormone sensitivity, and prognosis. (A) The detection rate of anti-Annexin A₂ antibody in children with PNS was 17.8%. (B) The hospital stay and urine protein content of children with PNS who tested positive (n=106) and negative (n=490) for anti-Annexin A₂ antibody. When immunosuppressants were administered, the level of Anti-Annexin A₂ antibody gradually reduced in the children with PNS (D) and was accompanied by a continuous decrease in the 24-hour urine protein level and an increase in serum albumin (C). PNS, primary nephrotic syndrome; HSPN, Henoch-Schonlein purpura nephritis; IgAN, IgA nephropathy; SH, simple hematuria or isolated hematuria; LN, lupus nephritis; NC, normal children; M-TP, total trace protein in the urine.

(Figure 2A). IgG was not locally co-localized in the glomerulus in normal control (Figure 2B). The eluted IgG reacted with both the Annexin A₂ protein band isolated from the kidney tissues and recombinant Annexin A₂ protein, and the addition of anti-IgG4 secondary antibody confirmed that the eluted anti-Annexin A₂ IgG antibodies contained the IgG4 subtype. These observations demonstrated that IgG antibodies against Annexin A₂, one of which was identified as the IgG4 subtype, exist on the surface of glomerular podocytes (Figure 2C).

Intravenous injection of anti-Annexin A₂ antibody can cause damage to podocytes and lead to proteinuria in BALB/c mice

To investigate whether intravenous injection of anti-Annexin antibody would cause damage to kidney tissues *in vivo* and lead to proteinuria, six male BALB/c mice were injected intravenously with rabbit polyclonal anti-Annexin A₂ antibody (ab41803, Abcam). The highest urine protein content observed at 48 hours after injection

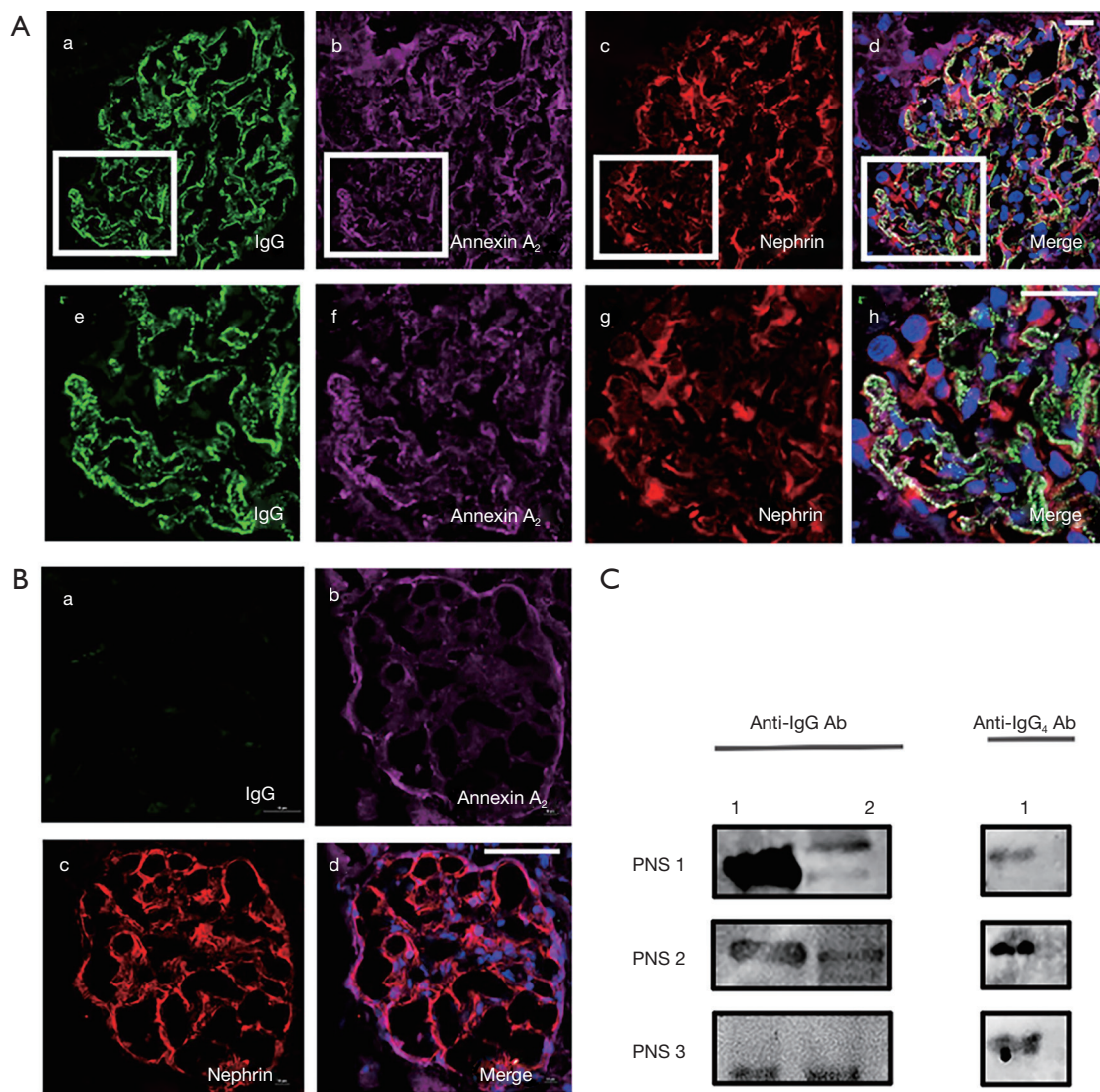


Figure 2 Autoantibody against glomerular podocyte annexin A₂ protein can be detected in the kidney tissues of children with PNS. (A) IgG in the glomerulus (a,e), Annexin A₂ expressed on podocytes (b,f), and nephrin expressed on the podocyte foot process slit diaphragm (c,g) could be locally co-localized in the glomeruli of children with PNS (d,h); (e-h) are enlarged images of the framed areas in (a-d), respectively. Scale bar of (a-d): 100 μ m, Scale bar of (e-h): 50 μ m. (B) Normal control. (a-d) Scale bar: 50 μ m. (C) The eluted IgG reacted with both the Annexin A₂ protein band isolated from the kidney tissues and recombinant Annexin A₂ protein, and the addition of anti-IgG₄ secondary antibody confirmed that the eluted anti-Annexin A₂ IgG antibodies included the IgG₄ subtype. 1, recombinant Annexin A₂ protein; 2, Annexin A₂ protein band isolated from total protein of human podocytes after SDS-PAGE. Indirect immunofluorescence method was used for staining.

(Figure 3A). Sensitization induced by the antibody was observed after 24 hours (Figure 3B) and was accompanied by proteinuria. Immunofluorescence detection revealed that intravenous injection of anti-Annexin A₂ antibody led to the downregulated expression of nephrin, WT-1, and ZO-1, and the upregulated expression of desmin in the glomeruli

of the BALB/c mice (Figure 3C). HE staining showed an increase in glomerular volume, a narrowed balloon space, and an opened capillary, and Masson staining showed a large amount of collagen exudation. TEM observation indicated local foot process fusion and basement membrane thickening in the glomerulus with no significant

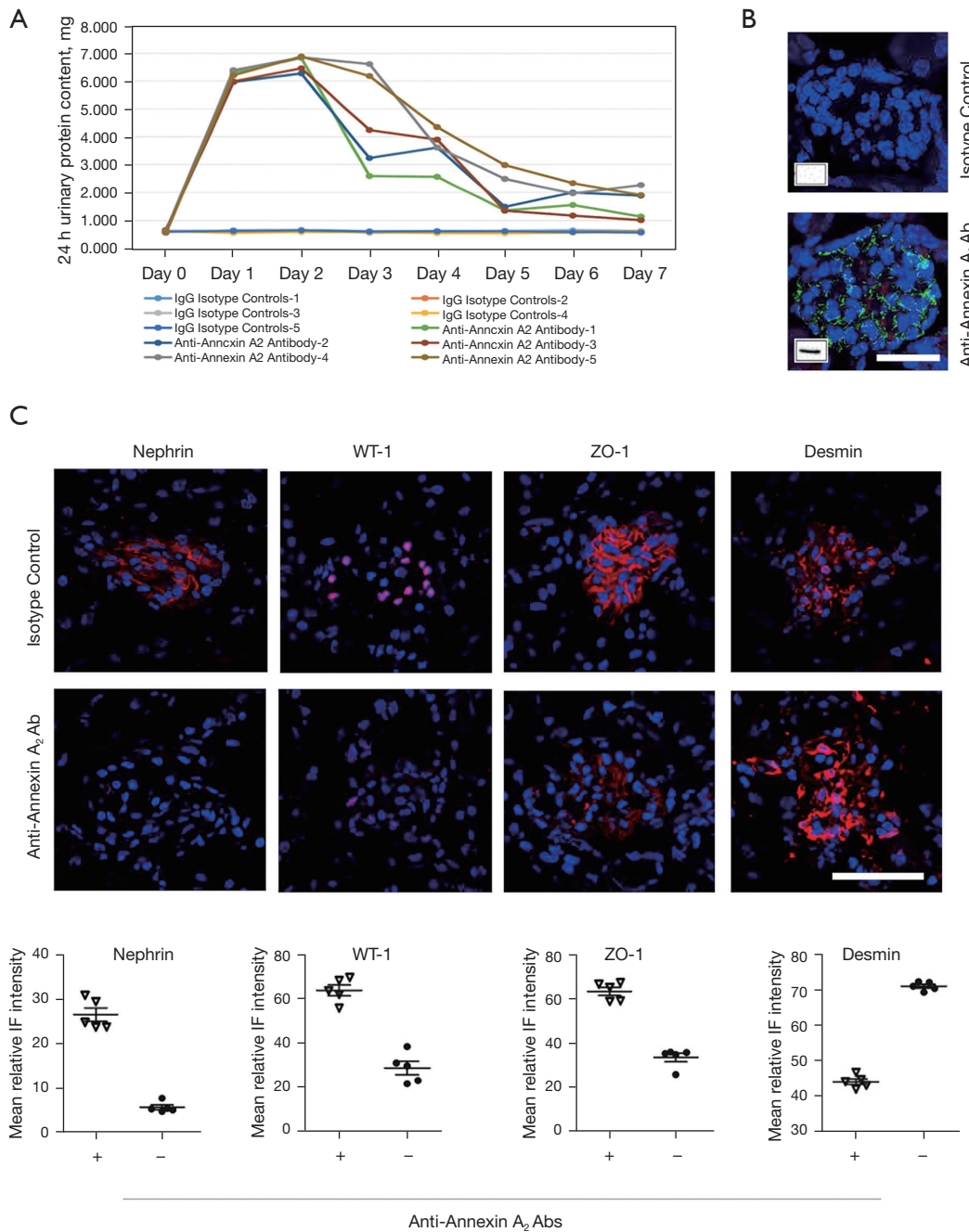


Figure 3 Intravenous injection of anti-Annexin A₂ antibody can cause podocyte injury and proteinuria in BALB/c mice. (A) Proteinuria was observed in BALB/c mice intravenously injected with rabbit polyclonal Annexin A₂ antibody. An equal amount of rabbit IgG polyclonal antibody-isotype was injected as a control. (B) Sensitization induced by rabbit polyclonal anti-Annexin A₂ antibody was observed in BALB/c mice at 24 hours after intravenous injection of the antibody, whereas no IgG antibodies were detected in the glomeruli of mice intravenously injected with an equal amount of rabbit IgG polyclonal antibody-isotype control. The small box in the lower left corner shows the western blotting results for the antibody eluted from the mouse glomeruli after reaction with recombinant Annexin A₂ protein. Scale bar: 50 μm. (C) Intravenous injection of anti-Annexin A₂ antibody into BALB/c mice led to the downregulation of nephrin, WT-1, and ZO-1, and the upregulation of desmin in the glomerulus. All P<0.05. Scale bar: 50 μm. Indirect immunofluorescence method was used for staining.

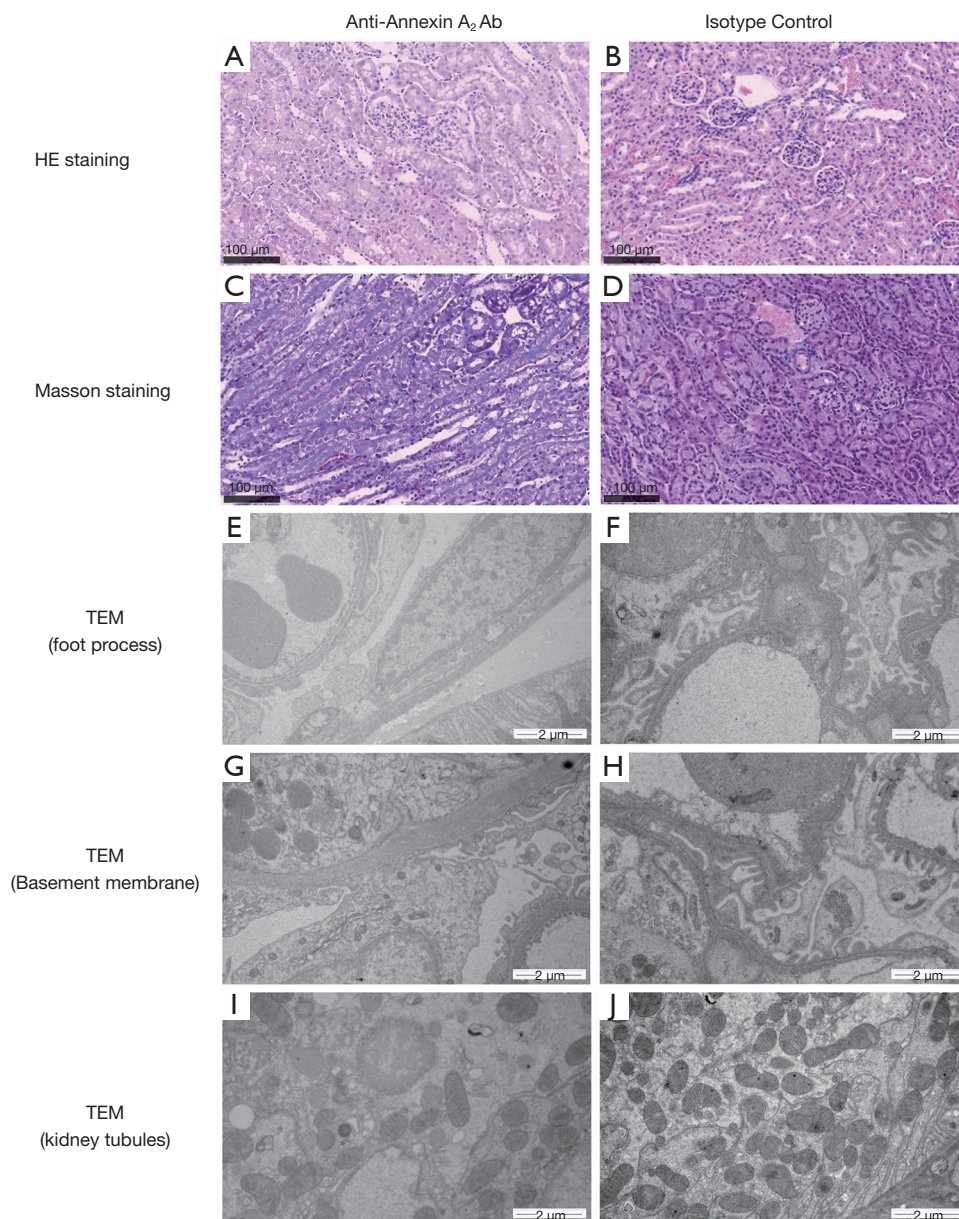


Figure 4 Intravenous injection of anti-Annexin A₂ antibody can cause podocyte injury in BALB/c mice. HE staining and Masson staining. Scale bar: 100 μm. TEM observation indicated local foot process fusion and basement membrane thickening in the glomerulus with no significant abnormalities observed in the kidney tubules. These changes were not observed in the control group. Scale bar: 2 μm. HE, hematoxylin-eosin; TEM, transmission electron microscopy.

abnormalities observed in the kidney tubules (*Figure 4*).

Anti-Annexin A₂ antibody can cause damage to podocyte functions

To further clarify its effect on podocytes, an anti-Annexin

A₂ antibody was added to podocyte culture medium. After culture, the adhesion (*Figure 5A*), migration (*Figure 5B*), and phagocytosis (*Figure 5C*) abilities of podocytes all showed a gradient reduction as the concentration of anti-Annexin A₂ antibody increased, and the structure of F-actin was destroyed (*Figure 5D*). Meanwhile, the levels of the

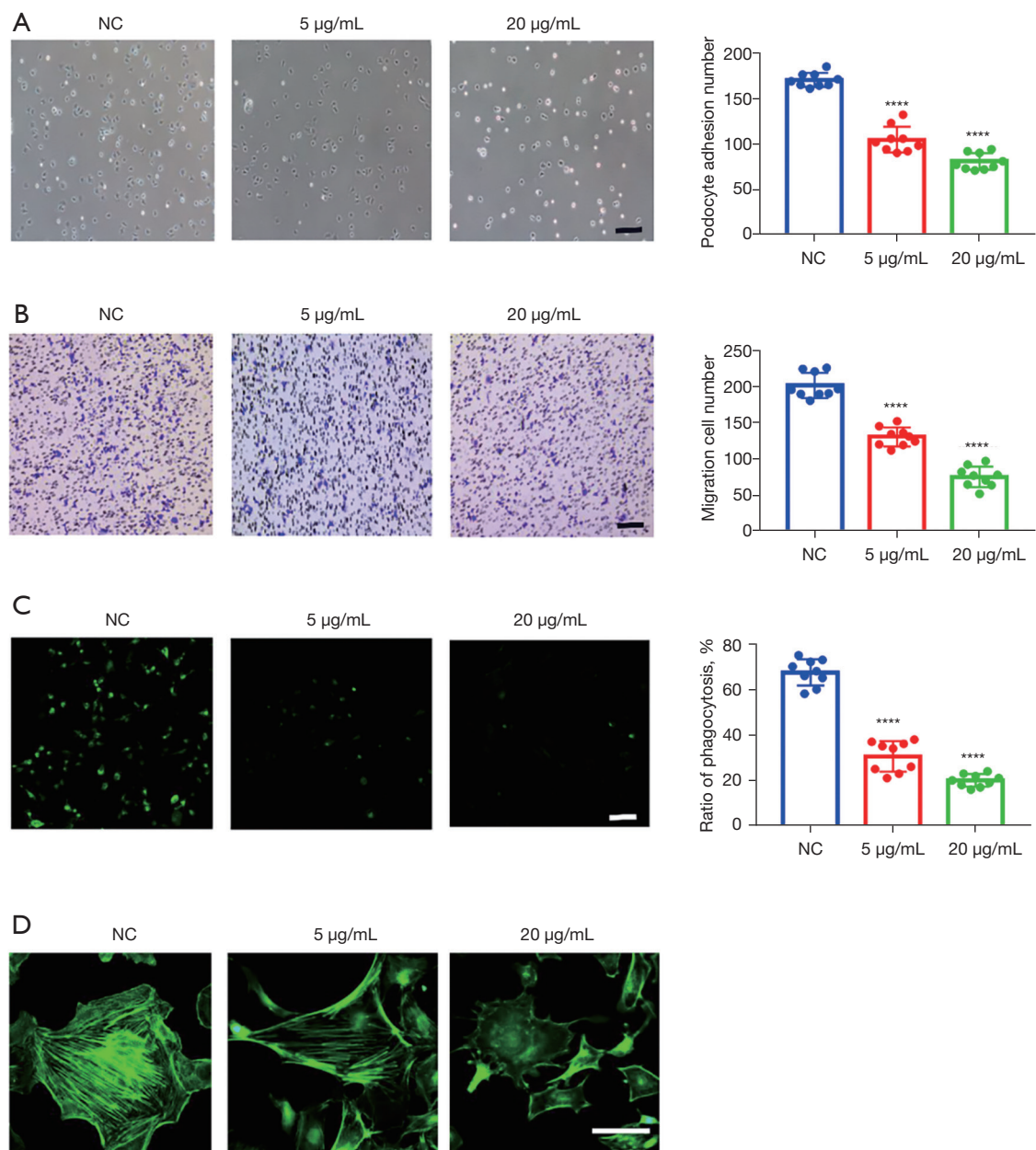


Figure 5 Anti-Annexin A₂ antibody can reduce podocyte function and morphology. The adhesion (A), migration (B), and phagocytosis (C) abilities of podocytes showed a gradient reduction as the concentration of anti-Annexin A₂ antibody in the podocyte culture medium increased. Scale bar: 100 µm. The structure of F-actin was also affected (D). Scale bar: 50 µm. ****, $P < 0.0001$. Podocyte adhesion number: the number of adherent cells in each well after treatment with anti-Annexin A₂ antibody; migration cell number: the number of cells that had migrated after treatment with anti-Annexin A₂ antibody; the ratio of phagocytosis: the proportion of cells that had phagocytosed FITC-transferrin after treatment with anti-Annexin A₂ antibody. NC, the normal control treatment in the functional assays was consistent with that in the experimental group except that no anti-annexin A₂ antibody was added. The cells were stained with 1% purple crystals (B). Indirect immunofluorescence method was used for staining (D).

key Rho signaling pathway molecules Cdc42 and Rac1/2/3 were decreased significantly, but no significant change was detected in the levels of RhoA (Figure 6A,6B). Further analysis revealed that Tyr24 phosphorylation of Annexin A₂ protein was enhanced (Figure 6C-6E).

Tyr24 hyperphosphorylation of Annexin A₂ can cause podocyte cytoskeleton rearrangement and functional damage

We next explored whether Tyr24 hyperphosphorylation of Annexin A₂ induced by the addition of anti-Annexin A₂ antibody to the podocyte culture medium can lead to podocyte cytoskeleton rearrangement and functional damage. Annexin A₂ Tyr24 was mutated to glutamic acid to simulate phosphorylation (Y24E) and to alanine to simulate dephosphorylation (Y24A), and these mutants were then overexpressed in podocytes. The experimental results showed that Tyr24 hyperphosphorylation of Annexin A₂ reduced the adhesion (Figure S3A), migration (Figure S3B), and phagocytosis (Figure S3C) ability of podocytes, and also induced podocyte cytoskeletal protein rearrangement (Figure S4) and led to a decrease in the expression and activities of Cdc42 and Rac1 (Figure 6F-6I). A co-immunoprecipitation assay was used to detect interaction between endogenous Annexin A₂ and protein tyrosine phosphatase 1 B (PTP1B) (Figure 6J). The results revealed that the interaction between PTP1B and Annexin A₂ decreased after the addition of anti-annexin A₂ antibody, especially with mutated Annexin A₂ (Y24E) (Figure 6K).

Anti-annexin A₂ antibody facilitates the intracellular transfer of Annexin A₂ on the surface of podocytes

After pre-treatment of podocytes with different concentrations of Annexin A₂ antibody, indirect immunofluorescence and western blotting were used to detect total Annexin A₂ and Annexin A₂ on the surface of podocytes at different times. The results showed that the Annexin A₂ protein in podocytes gradually translocated from the surface of the cell membrane to the inside of the cell as the concentration of Annexin A₂ antibody and the incubation time increased (Figure 7).

Discussion

Annexin A₂ antibody has been reported in patients with lupus nephritis (30), Behçet's disease (31), and anti-

phospholipid antibodies (32). However, except for adult membranous nephropathy, which is believed to be related to autoantibodies, no recognized autoantibodies have been identified in other kidney diseases. Therefore, the present study is the first to examine the presence of Annexin A₂ autoantibodies in children with nephrotic syndrome.

As a member of the multigene family of annexins, Annexin A₂ consists of 339 amino acids with a molecular weight of 36 kD. Its molecular structure comprises a 33-kD C-terminal domain and a 3-kD N-terminal domain (33). The C-terminal domain contains four homologous repeats, each of which consists of 70 amino acids in an α -helix that constitutes a conservative disc-like structure, which allows them to bind to calcium ions, phospholipids, and F-actin (34); this suggests that Annexin A₂ has great significance to cytoskeletal rearrangement and various membrane-related changes. In the present study, experiments showed that the autoantibody against Annexin A₂ protein could affect the rearrangement of podocyte cytoskeleton proteins by acting upon Annexin A₂ protein, thereby causing damage to podocyte functions and eventually inducing proteinuria.

The cytoskeleton in podocytes is subject to the precise regulation by many molecules. The small GTPases of the Rho family, particularly RhoA, Rac1, and Cdc42, can transmit molecular signals from membrane proteins to F-actin and are widely recognized as molecular switches for the cytoskeletal regulatory process. Moore *et al.* reported that knockdown of Annexin A₂ via RNA interference significantly reduced Rho protein activity and decreased the formation of F-actin bundles at cell lamellipodia, thus inhibiting cell invasion and migration (29). Similarly, in the present study, decreases were observed mainly in Cdc42 and Rac1, and their activities were simultaneously reduced, after knockdown of Annexin A₂ in podocytes via RNA interference. In contrast, no significant changes in the expression and activity of RhoA were observed. Studies have shown that Rac1 and Cdc42 can regulate the formation of filopodia and lamellipodia, respectively, and thus affect cell movement (35). Meanwhile, RhoA can promote the formation of somatic and terminal actin-myosin tonofilaments (35). Clinical studies have found that activity changes and abnormal expression of these three molecules can lead to proteinuria (36,37). Therefore, it is by downregulating the expression and activities of Cdc42 and Rac1, as key molecules in the Rho/ROCK signaling pathway, that the autoantibody against Annexin A₂ protein causes proteinuria.

Rescher *et al.* demonstrated that tyrosine phosphorylation

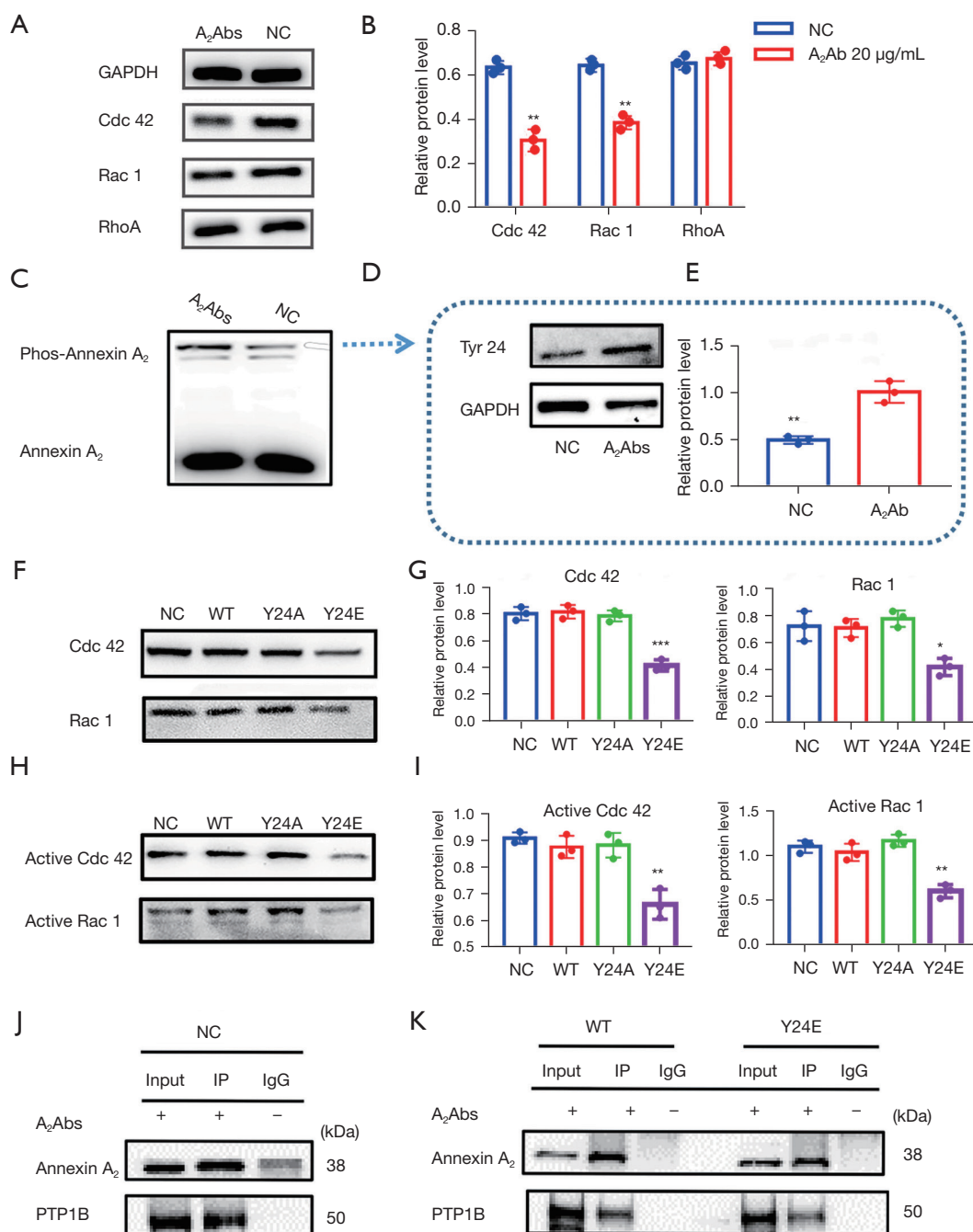


Figure 6 Anti-annexin A₂ antibody leads to increased Tyr24 phosphorylation of Annexin A₂, impairing the cytoskeleton signaling pathway. Anti-Annexin A₂ antibody impairs the cytoskeleton signaling pathway (A,B). Anti-Annexin A₂ antibody (20 µg/mL) was added to the podocyte medium and cultured for 24 hours, which deepened the color of one of the phosphorylated Annexin A₂ bands (C); hybridization of this band with a monoclonal antibody indicated it to be Annexin A₂ protein with phosphorylated Tyr24 (D,E). Tyr24 hyperphosphorylation of Annexin A₂ in podocytes led to a decrease in the expression (F,G) and activities (H,I) of the key Rho-associated kinase signaling pathway molecules Cdc42 and Rac1. *, P<0.05; **, P<0.01; ***, P<0.001. Lysates from MPC5 cells (NC) immunoprecipitated after being treated with anti-Annexin A₂ antibody or an isotype-matched control IgG were analyzed by western blotting (J). MPC5 cells transfected with Annexin A₂ (WT) or Y24E mutant Annexin A₂ (Y24E) were subjected to immunoprecipitation after being treated with anti-Annexin A₂ antibody or an isotype-matched control IgG, followed by western blot analysis (K).

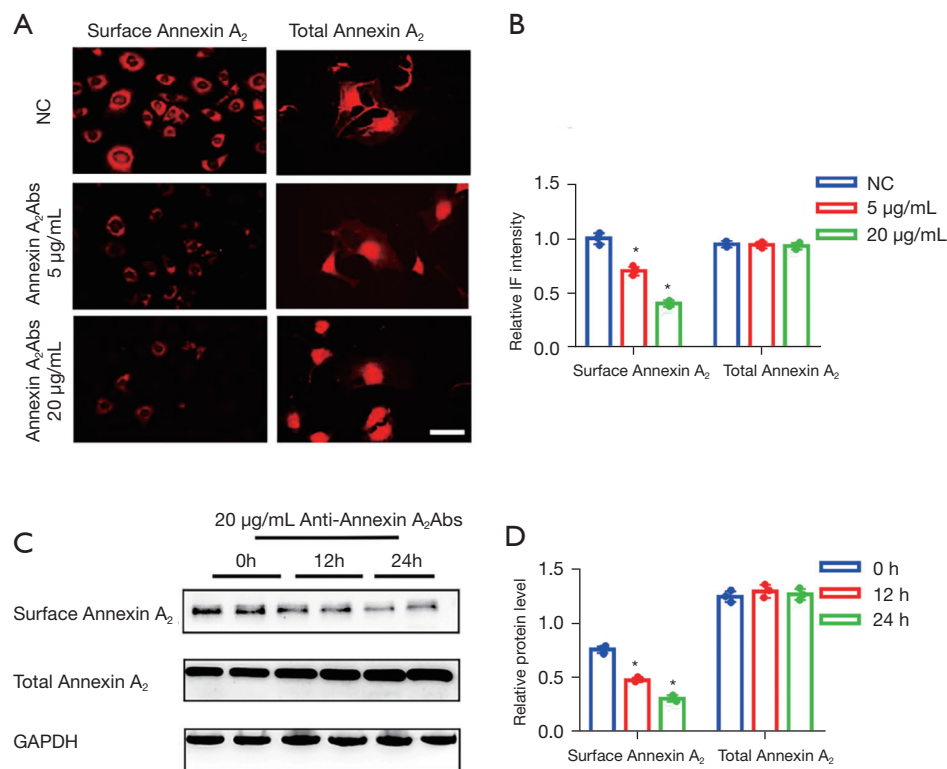


Figure 7 Annexin A₂ antibody affects the distribution of Annexin A₂ protein in podocytes. The Annexin A₂ protein in podocytes gradually translocated from the surface of the cell membrane to the inside of the cell as the Annexin A₂ antibody concentration increased (A,B), and this trend increased with the length of incubation time (C,D). Scale bar: 50 µm. *, P<0.05. Indirect immunofluorescence method was used for staining.

of Annexin A₂ may be key to the initiation of Rho-dependent actin-mediated cell adhesion reduction and matrix detachment in baby hamster kidney (BHK) cells upon insulin stimulation (27). Studies by de Graauw *et al.* (38) and Hayes *et al.* (39) confirmed that tyrosine phosphorylation of Annexin A₂ can induce cytoskeletal rearrangement and promote cell transformation and tube formation. In a cell model based on tyrosine-phosphorylated growth factor signaling, the tyrosine of Annexin A₂ was found to be phosphorylated after insulin receptor activation. Phosphorylation occurs prior to the accumulation of peripheral actin and subsequent cell separation. All of these morphological changes require the tyrosine-phosphorylated Rho signaling at the downstream of Annexin A₂ and can, in turn, be suppressed with the consumption of Annexin A₂. More importantly, in the studies mentioned above, in the absence of upstream signal stimulation, mutants mimicking phosphorylated Annexin A₂ could still promote cytoskeletal rearrangement and alter the cell phenotype. Therefore, as a

connection between the membrane and actin cytoskeletons, Annexin A₂ is involved in signal transduction and plays a vital role in life activities, such as cell transformation, adhesion, and movement. Besides, the tyrosine phosphorylation switches in Annexin A₂ function as the key point triggering Rho-dependent pathways related to cell adhesion control as well as actin-mediated cell morphological changes (27). In our research, the Tyr24 phosphorylation level of Annexin A₂ was significantly increased following the addition of the anti-Annexin A₂ antibody. Existing studies have found that Tyr23 phosphorylation of Annexin A₂ can regulate RhoA-mediated actin rearrangement and cell adhesion (27). However, no reports have been published on the effects of Tyr24 phosphorylation of Annexin A₂. Therefore, to further elucidate whether the increase in Tyr24 phosphorylation induced by anti-Annexin A₂ antibody is responsible for triggering the Rho-dependent pathway, we employed the amino acid point mutation technique to mimic Tyr24 phosphorylation and Tyr24 dephosphorylation

to overexpress Annexin A₂ in podocytes. Our findings suggested that, in contrast to Tyr23 phosphorylation of Annexin A₂, which caused cytoskeletal rearrangement by upregulating RhoA, Tyr24 hyperphosphorylation of Annexin A₂ did not affect RhoA but triggered podocyte cytoskeletal rearrangement by downregulating the contents and activities of the Rho family members Rac1 and Cdc42, resulting in podocyte function damage. The co-immunoprecipitation assay results suggest that Annexin A₂ autoantibody binding to Annexin A₂ affects the binding of Annexin A₂ to PTP1B, thereby weakening PTP1B dephosphorylation, resulting in excessive Annexin A₂ phosphorylation. To sum up, through promoting Tyr24 phosphorylation of Annexin A₂, the Annexin A₂ antibody imposes its effect on the Rho signaling pathway and induces podocyte rearrangement, resulting in podocyte damage and ultimately leading to proteinuria and PNS.

Our study results show that, like patients with anti-neutrophil cytoplasmic autoantibody -related vasculitis, these PNS patients with Annexin A₂ autoantibody showed no deposition of immune or oligo-immune complexes in the glomerulus. Further, these patients did not have a large amount of immune complex deposition in the glomerulus like in adult membranous nephropathy. Our study showed that Annexin A₂ antibody directly binds to the Annexin A₂ protein on the surface of podocytes, damaging the podocytes and exerting a pathogenic effect. Other than the classic mechanism by which an attacking complex which damages cells is formed through complement activation after the antibody binds to the antigen to form an immune complex, many other mechanisms play a role in PNS. These mechanisms include the direct binding with the antigen on the cell surface. This combination of antigen and antibody is different from that in adult membranous nephropathy as there is no linear immune complex deposition in the glomerulus; instead, sensitized Annexin A₂ antibody can be detected on the surface of glomerular podocytes. Since Annexin A₂ is distributed in dots on the surface of podocytes, the Annexin A₂ antibody detected is also distributed in dots.

In conclusion, Annexin A₂ autoantibody can be detected in some children with nephrotic syndrome without genetic factors and is associated with patient outcome. Both *in vivo* and *in vitro* experiments have proved that the antibody is pathogenic. Therefore, we speculate that Annexin A₂ autoantibody may be involved in the etiology of some children with nephrotic syndrome caused by autoimmune factors.

Acknowledgments

We are grateful to all of the study participants and their families, and to the physicians who treated them. We also want to thank the Zhejiang Provincial Key Laboratory of Immunity and Inflammatory Diseases for its support.

Funding: This study was supported by the Key Project of Provincial Ministry Co-Construction, Health Science and Technology Project Plan of Zhejiang Province (grant No. WKJ-ZJ-2128), the Key Laboratory of Women's Reproductive Health Research of Zhejiang Province (grant No. ZDFY2020-RH-0006), the National Natural Science Foundation of China (grant Nos. 81501760, 81470939, 81270792, and 81170664), and the Key Research and Development Plan of Zhejiang Province (grant No. 2019C03028).

Footnote

Reporting Checklist: The authors have completed the ARRIVE reporting checklist. Available at <https://dx.doi.org/10.21037/atm-21-3988>

Data Sharing Statement: Available at <https://dx.doi.org/10.21037/atm-21-3988>

Conflicts of Interest: All authors have completed the ICMJE uniform disclosure form (available at <https://dx.doi.org/10.21037/atm-21-3988>). The authors have no conflicts of interest to declare.

Ethical Statement: The authors are accountable for all aspects of the work in ensuring that questions related to the accuracy or integrity of any part of the work are appropriately investigated and resolved. All procedures in this study involving human participants were performed in accordance with the Declaration of Helsinki (as revised in 2013). The Ethics Committee of the Children's Hospital of Zhejiang University School of Medicine approved the study (2019-IRB-139). Informed consent was obtained from the parents/guardians of each patient after a full explanation of the purpose of this study had been given. All animal experiments were performed under a project license (No. 20744) granted by Zhejiang University School of Medicine, and in compliance with the national guidelines for the care and use of animals.

Open Access Statement: This is an Open Access article

distributed in accordance with the Creative Commons Attribution-NonCommercial-NoDerivs 4.0 International License (CC BY-NC-ND 4.0), which permits the non-commercial replication and distribution of the article with the strict proviso that no changes or edits are made and the original work is properly cited (including links to both the formal publication through the relevant DOI and the license). See: <https://creativecommons.org/licenses/by-nc-nd/4.0/>.

References

- Roth KS, Amaker BH, Chan JC. Nephrotic syndrome: pathogenesis and management. *Pediatr Rev* 2002;23:237-48.
- Noone DG, Iijima K, Parekh R. Idiopathic nephrotic syndrome in children. *Lancet* 2018;392:61-74.
- Vivarelli M, Massella L, Ruggiero B, et al. Minimal Change Disease. *Clin J Am Soc Nephrol* 2017;12:332-45.
- Banerjee S. Steroid resistant nephrotic syndrome. *Indian J Pediatr* 2002;69:1065-9.
- Trautmann A, Schnaidt S, Lipska-Ziętkiewicz BS, et al. Long-Term Outcome of Steroid-Resistant Nephrotic Syndrome in Children. *J Am Soc Nephrol* 2017;28:3055-65.
- Gipson DS, Chin H, Presler TP, et al. Differential risk of remission and ESRD in childhood FSGS. *Pediatr Nephrol* 2006;21:344-9.
- Paik KH, Lee BH, Cho HY, et al. Primary focal segmental glomerular sclerosis in children: clinical course and prognosis. *Pediatr Nephrol* 2007;22:389-95.
- Martinelli R, Okumura AS, Pereira LJ, et al. Primary focal segmental glomerulosclerosis in children: prognostic factors. *Pediatr Nephrol* 2001;16:658-61.
- Mekahli D, Liutkus A, Ranchin B, et al. Long-term outcome of idiopathic steroid-resistant nephrotic syndrome: a multicenter study. *Pediatr Nephrol* 2009;24:1525-32.
- Ali AA, Wilson E, Moorhead JF, et al. Minimal-change glomerular nephritis. Normal kidneys in an abnormal environment? *Transplantation* 1994;58:849-52.
- Li J, Wang L, Wan L, et al. Mutational spectrum and novel candidate genes in Chinese children with sporadic steroid-resistant nephrotic syndrome. *Pediatr Res* 2019;85:816-21.
- Shalhoub RJ. Pathogenesis of lipoid nephrosis: a disorder of T-cell function. *Lancet* 1974;2:556-60.
- Saleem MA, Kobayashi Y. Cell biology and genetics of minimal change disease. *F1000Res* 2016. doi: 10.12688/f1000research.7300.1.
- Koyama A, Fujisaki M, Kobayashi M, et al. A glomerular permeability factor produced by human T cell hybridomas. *Kidney Int* 1991;40:453-60.
- Cunard R, Kelly CJ. T cells and minimal change disease. *J Am Soc Nephrol* 2002;13:1409-11.
- Grimbert P, Audard V, Remy P, et al. Recent approaches to the pathogenesis of minimal-change nephrotic syndrome. *Nephrol Dial Transplant* 2003;18:245-8.
- Mathieson PW. Immune dysregulation in minimal change nephropathy. *Nephrol Dial Transplant* 2003;18 Suppl 6:vi26-9.
- Bertelli R, Bonanni A, Di Donato A, et al. Regulatory T cells and minimal change nephropathy: in the midst of a complex network. *Clin Exp Immunol* 2016;183:166-74.
- Colucci M, Carsetti R, Cascioli S, et al. B cell phenotype in pediatric idiopathic nephrotic syndrome. *Pediatr Nephrol* 2019;34:177-81.
- Printza N, Papachristou F, Tzimouli V, et al. Peripheral CD19+ B cells are increased in children with active steroid-sensitive nephrotic syndrome. *NDT Plus* 2009;2:435-6.
- Mundel P, Shankland SJ. Podocyte biology and response to injury. *J Am Soc Nephrol* 2002;13:3005-15.
- Brinkkoetter PT, Ising C, Benzing T. The role of the podocyte in albumin filtration. *Nat Rev Nephrol* 2013;9:328-36.
- Debiec H, Ronco P. PLA2R autoantibodies and PLA2R glomerular deposits in membranous nephropathy. *N Engl J Med* 2011;364:689-90.
- Jamin A, Berthelot L, Couderc A, et al. Autoantibodies against podocytic UCHL1 are associated with idiopathic nephrotic syndrome relapses and induce proteinuria in mice. *J Autoimmun* 2018;89:149-61.
- Meyer TN, Schwesinger C, Wahlefeld J, et al. A new mouse model of immune-mediated podocyte injury. *Kidney Int* 2007;72:841-52.
- Zhu X, Ye Y, Xu C, et al. Protein phosphatase 2A modulates podocyte maturation and glomerular functional integrity in mice. *Cell Commun Signal* 2019;17:91.
- Rescher U, Ludwig C, Konietzko V, et al. Tyrosine phosphorylation of annexin A2 regulates Rho-mediated actin rearrangement and cell adhesion. *J Cell Sci* 2008;121:2177-85.
- Zheng L, Foley K, Huang L, et al. Tyrosine 23 phosphorylation-dependent cell-surface localization of annexin A2 is required for invasion and metastases of pancreatic cancer. *PLoS One* 2011;6:e19390.
- Moore AW, McInnes L, Kreidberg J, et al. YAC complementation shows a requirement for Wt1 in the

- development of epicardium, adrenal gland and throughout nephrogenesis. *Development* 1999;126:1845-57.
30. Caster DJ, Korte EA, Merchant ML, et al. Autoantibodies targeting glomerular annexin A2 identify patients with proliferative lupus nephritis. *Proteomics Clin Appl* 2015;9:1012-20.
 31. Chen P, Yan H, Tian Y, et al. Annexin A2 as a target endothelial cell membrane autoantigen in Behçet's disease. *Sci Rep* 2015;5:8162.
 32. Salle V, Mazière JC, Brulé A, et al. Antibodies against the N-terminal domain of annexin A2 in antiphospholipid syndrome. *Eur J Intern Med* 2012;23:665-8.
 33. Bharadwaj A, Bydoun M, Holloway R, et al. Annexin A2 heterotetramer: structure and function. *Int J Mol Sci* 2013;14:6259-305.
 34. Hayes MJ, Shao D, Bailly M, et al. Regulation of actin dynamics by annexin 2. *EMBO J* 2006;25:1816-26.
 35. Raftopoulou M, Hall A. Cell migration: Rho GTPases lead the way. *Dev Biol* 2004;265:23-32.
 36. Wang L, Ellis MJ, Gomez JA, et al. Mechanisms of the proteinuria induced by Rho GTPases. *Kidney Int* 2012;81:1075-85.
 37. Huang Z, Zhang L, Chen Y, et al. Cdc42 deficiency induces podocyte apoptosis by inhibiting the Nwasp/stress fibers/YAP pathway. *Cell Death Dis* 2016;7:e2142.
 38. de Graauw M, Tijdens I, Smeets MB, et al. Annexin A2 phosphorylation mediates cell scattering and branching morphogenesis via cofilin Activation. *Mol Cell Biol* 2008;28:1029-40.
 39. Hayes MJ, Moss SE. Annexin 2 has a dual role as regulator and effector of v-Src in cell transformation. *J Biol Chem* 2009;284:10202-10.

(English Language Editor: J. Reynolds)

Cite this article as: Ye Q, Zhang Y, Zhuang J, Bi Y, Xu H, Shen Q, Liu J, Fu H, Wang J, Feng C, Tang X, Liu F, Gu W, Zhao F, Zhang J, Qin Y, Shang S, Shen H, Chen X, Shen H, Liu A, Xia Y, Lu Z, Shu Q, Mao J. The important roles and molecular mechanisms of annexin A2 autoantibody in children with nephrotic syndrome. *Ann Transl Med* 2021;9(18):1452. doi: 10.21037/atm-21-3988

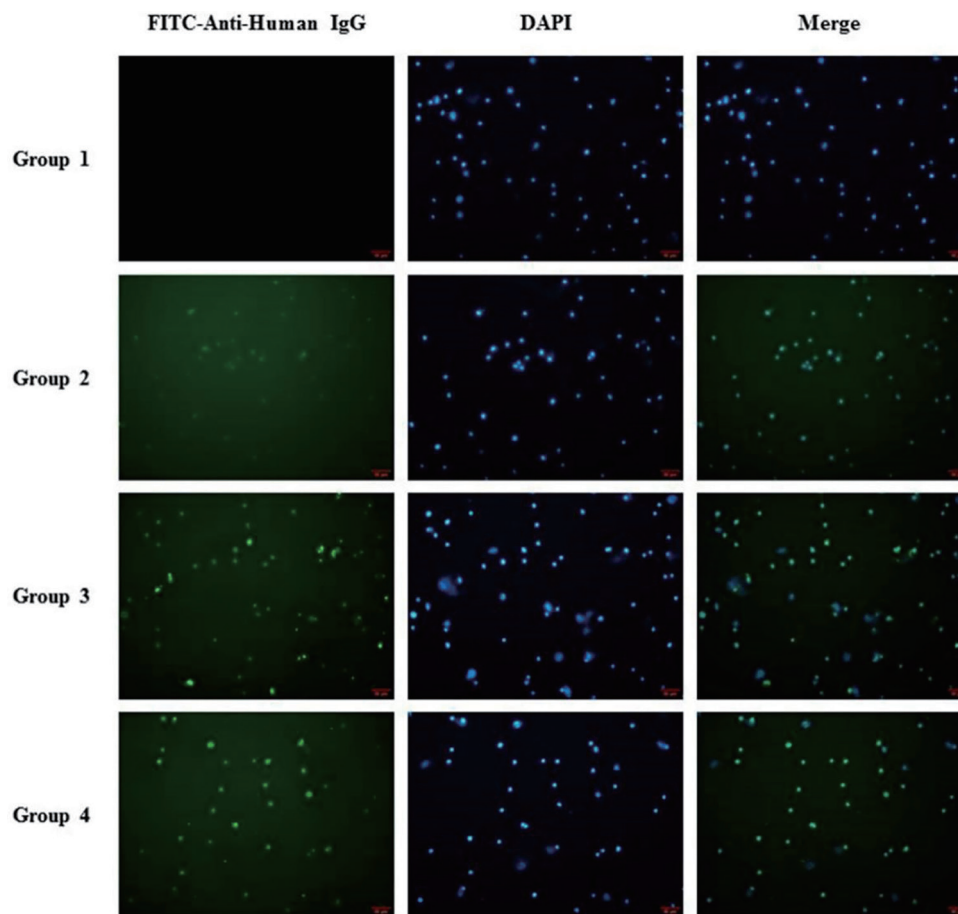


Figure S1 IgG-type autoantibody specific against human podocytes can be found in the serum of children with PNS. IgG antibodies purified from the serum of 20 children with PNS, serving as the primary antibody, were incubated with human podocytes and then rinsed with PBS. FITC-labeled monkey anti-human IgG (1:100 dilution) was added as the secondary antibody, followed by incubation for 1 hour at room temperature, rinsing, and observation and photographing under an inverted fluorescent microscope. Group 1: blank control (primary antibody: no serum added); group 2: negative serum control (primary antibody: healthy human serum); group 3: serum from a child with PNS with IgG-type autoantibody specific against podocytes as the primary antibody (initial concentration); group 4: serum from a child with PNS with IgG-type autoantibody specific against podocytes as the primary antibody (1:10 dilution). Scale bar: 50 μ m. Indirect immunofluorescence method was used for staining.

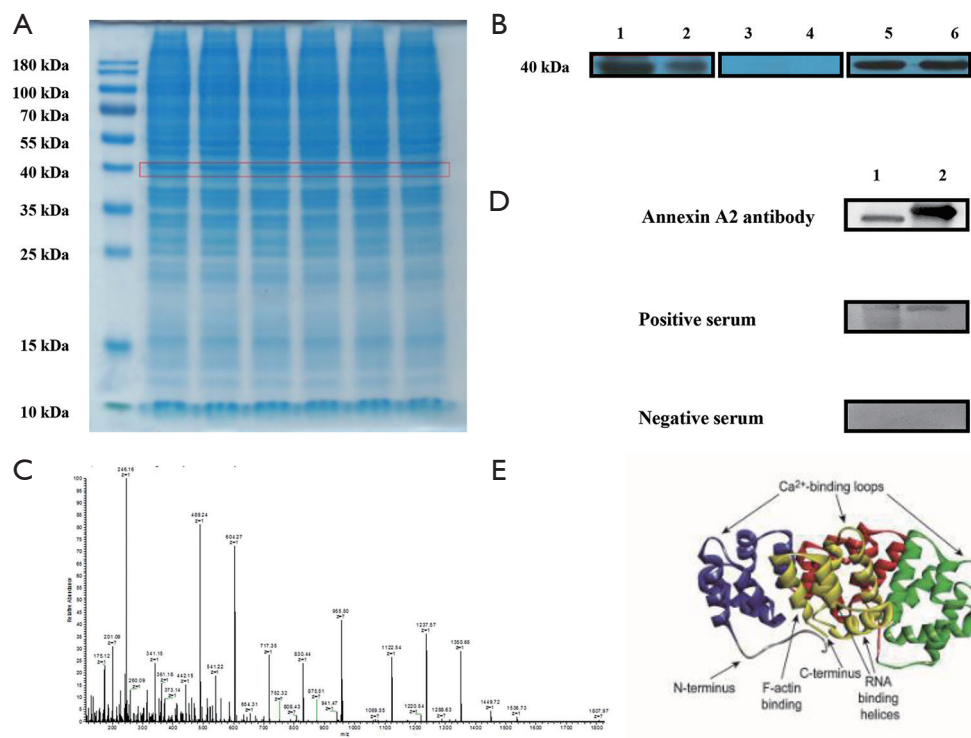


Figure S2 Annexin A₂ in podocytes is the main target antigen of the autoantibody in children with PNS. For the total protein of human podocytes, two sets of SDS-PAGE were conducted in parallel, one of which was used for Coomassie Brilliant Blue staining (A) and the other transferred to a nitrocellulose membrane after gel electrophoresis, to which serum from children with PNS was added (the presence of IgG autoantibody against podocytes had been verified via mouse podocyte immunofluorescence) for western blotting detection. Coomassie Brilliant Blue-stained bands corresponding to western blotting positive bands (B) were selected for mass spectrometry to identify Annexin A₂ protein (C). The commercial recombinant Annexin A₂ protein specifically reacted with serum from children with PNS containing Annexin A₂ antibody, and the commercial Annexin A₂ antibody also specifically reacted with the Annexin A₂ protein band isolated from human podocyte total protein after SDS-PAGE (D). (B) (1: 1,000-fold diluted IgG antibodies purified from the serum of PNS children; 2: 2000-fold diluted IgG antibodies purified from the serum of PNS children; 3: 1,000-fold diluted IgG antibodies purified from the serum of healthy people; 4: 2000-fold diluted IgG antibodies purified from the serum of healthy people; 5-6: β-actin). (D) (1: Annexin A₂ protein band isolated from human podocyte total protein after SDS-PAGE; 2: Recombinant Annexin A₂ protein; Positive serum: Serum containing Annexin A₂ antibody collected from children with PNS; Negative serum: serum collected from healthy people). (E) The three-dimensional structure of the Annexin A₂ protein.

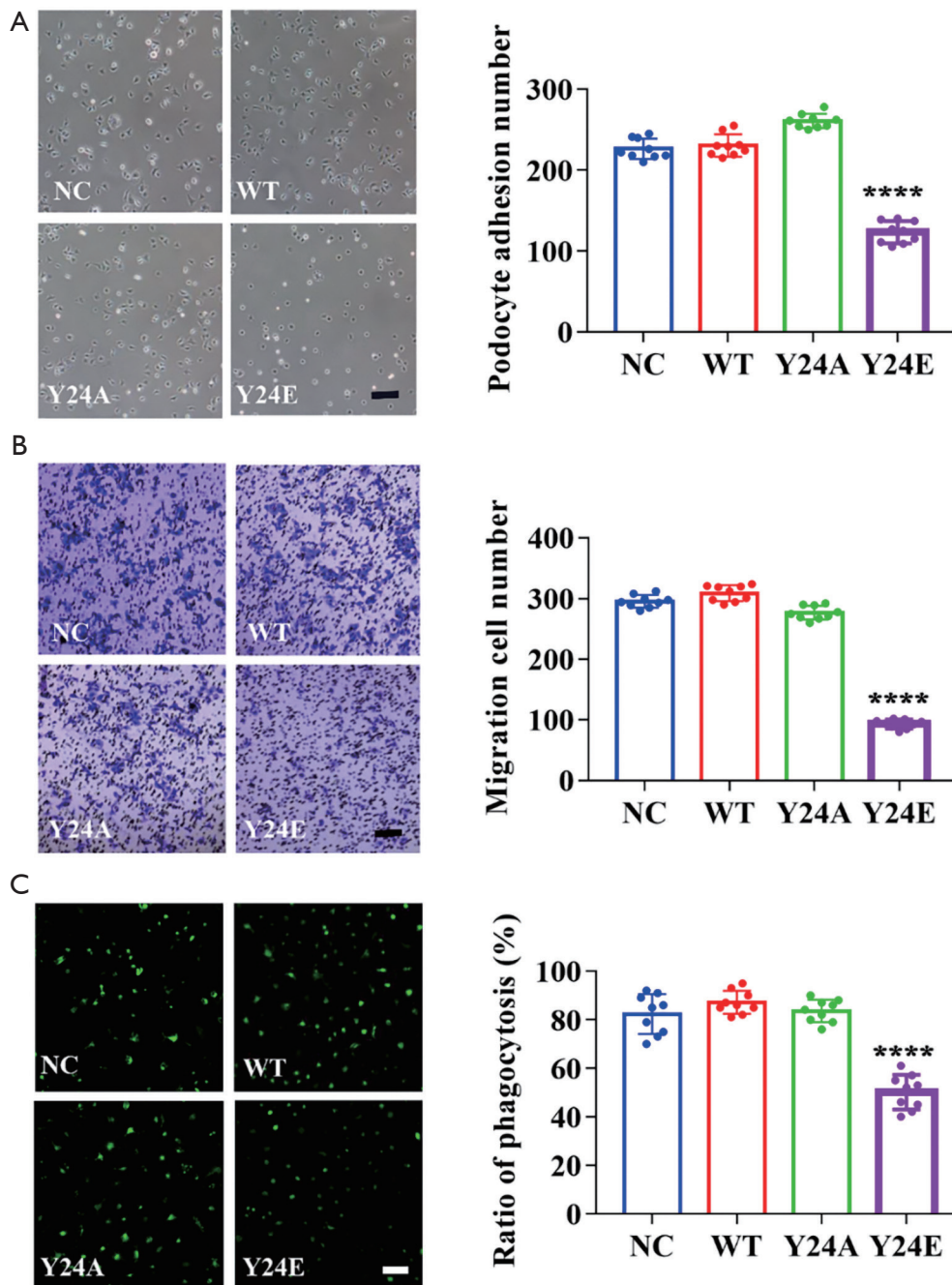


Figure S3 Tyr24 hyperphosphorylation of Annexin A₂ in podocytes can affect podocyte function. Tyr24 hyperphosphorylation of Annexin A₂ in podocytes can reduce the adhesion (A), migration (B) and phagocytosis (C) ability of podocytes. Scale bar: 100 μ m. ****, $P < 0.0001$. Migration ability was detected by Coomassie Brilliant Blue staining. Phagocytosis ability was detected by indirect immunofluorescence staining.

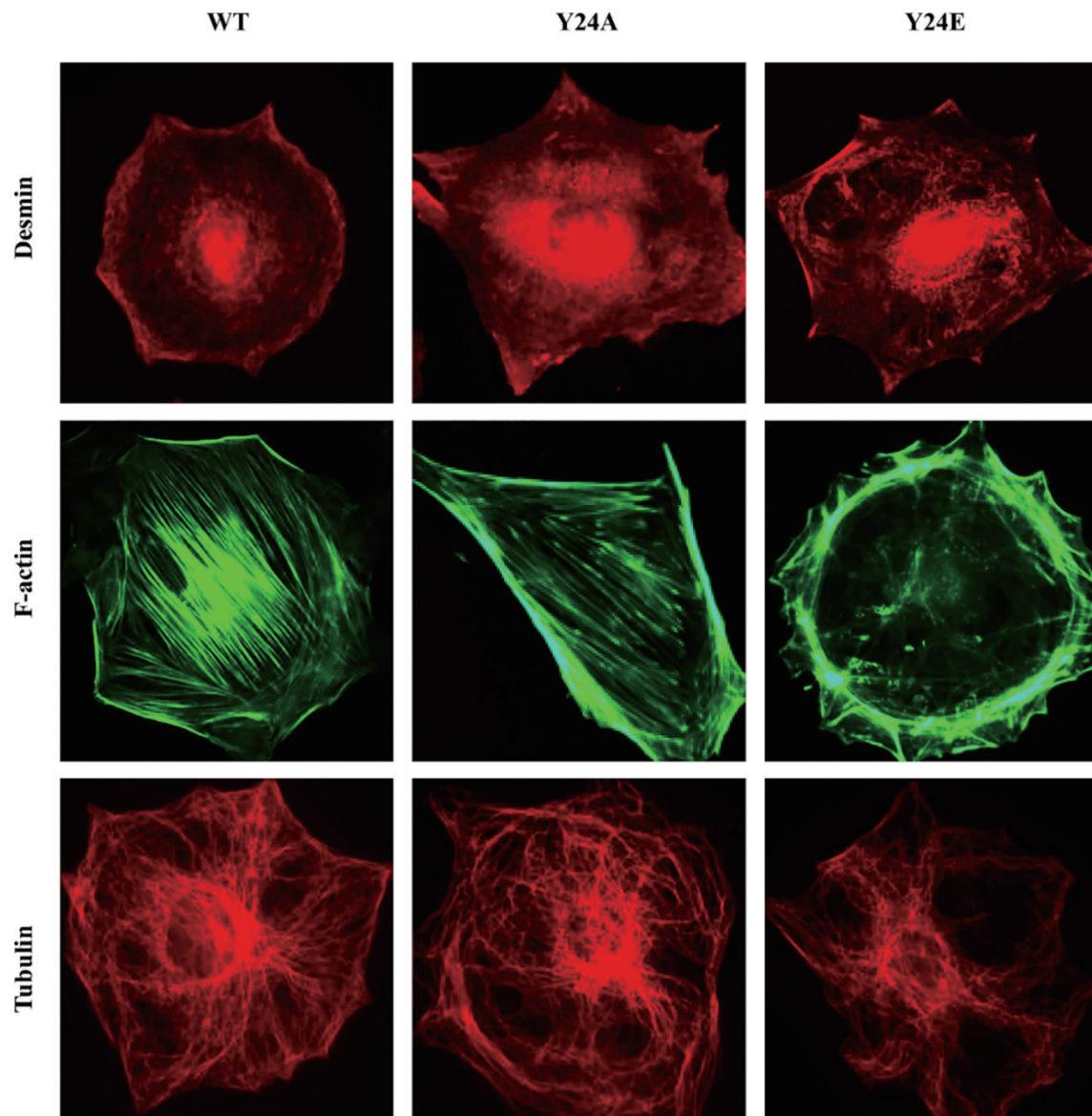


Figure S4 Tyr24 hyperphosphorylation of Annexin A₂ in podocytes can cause podocyte cytoskeletal changes. Indirect immunofluorescence method was used for staining. 600 X optical magnification.